SYNTHESIS OF MULTIPLE-PATTERN PLANAR ANTENNA ARRAYS WITH SINGLE PREFIXED OR JOINTLY OPTIMIZED AMPLITUDE DISTRIBUTIONS

J. Brégains, A. Trastoy, F. Ares, E. Moreno

Grupo de Sistemas Radiantes, Departamento de Física Aplicada,

Facultad de Física, Universidad de Santiago de Compostela

15782 Santiago de Compostela, SPAIN

E-mail: faares@usc.es

Fax: +34 981547046

Key words: planar arrays, synthesis of multiple patterns with a common amplitude distribution

ABSTRACT: Previous work on the generation of multiple radiation patterns by a single linear array antenna with an unchanging excitation amplitude distribution is generalized to planar arrays. The amplitude distribution common to all the excitation distributions can be prefixed or optimized jointly with the phase distributions.

1. INTRODUCTION

Since the size of antennas is fixed by physical considerations, the difficulty of accommodating them on satellites and other facilities with multiple antenna-based functions grows with the number of such functions if a separate antenna is used for each. In this context it is desirable for a single antenna to be able to generate multiple radiation patterns, with the excitation corresponding to each being selectable by suitable switching devices. However, it is also desirable for the various excitation patterns delivered to a multiple-pattern array antenna to have a common amplitude distribution, since implementation is technically more difficult for a variable amplitude distribution than for a variable phase distribution.

Previous papers from our group have described the synthesis of linear multiple-pattern array antennas in which the amplitude distribution common to all the excitations was prefixed so as to ensure smoothness [1] or was optimized jointly with the various excitation phase distributions [2]. In the latter case excitations were optimized directly, in the former a modified Woodward-Lawson approach was used. The direct optimization method is here generalized, for both prefixed and jointly optimized amplitudes, to planar array antennas, for which the joint optimization problem has previously been approached by Bucci et al. [3] using projection operators in pattern space.

2. DESCRIPTION OF THE METHOD

The array factor $F(\theta,\varphi)$ of an $N\times M$ rectangular array of radiating elements laid out in the (x,y) plane with its centre at the origin and its m and n axes coinciding with the x and y axes, respectively, is given by

$$F(\theta,\varphi) = \sum_{m=1}^{M}\sum_{n=1}^{N} I_{mn} \exp\left\{ jk \sin\theta\left(x_{mn}\cos\varphi + y_{mn}\sin\varphi\right)\right\} \quad (1)$$

where I_{mn} is the relative excitation of the mn-th element (located at (x_{mn},y_{mn})), $k=2\pi/\lambda$ is the wavenumber, and θ and φ are the usual polar coordinates. Given a prefixed distribution of excitation amplitudes $|I_{mn}|$ and the required characteristics of P target patterns (e.g. sidelobe levels, directivity, ripple, etc.), the excitation phase distribution corresponding to each pattern p is determined using simulated annealing [4] to vary the NM element phases so as to minimize a cost function constructed from the pattern specifications. For example, if only maximum sidelobe level and ripple are of interest for pattern p, a suitable cost function is

$$C_p = c_p\left(SLL_{pd} - SLL_p\right)^2 + d_p\left(R_{pd} - R_p\right)^2 \quad (2)$$

where the first term represents the deviation of the maximum side lobe level SLL_p from the desired level SLL_{pd} in the out-of-beam region (region A in the examples shown in Fig.1), and the second does likewise for the ripple level R_p at the top of the beam (region C in Fig.1). The constant weights c_p and d_p control the relative importance of the pattern quality goals.

If the excitation amplitude distribution is not prefixed but is nevertheless to be the same for all patterns, the optimization process varies the NM element amplitudes and the NMP phases all together. The cost function C is the sum of terms like the C_p of eq.2, and will generally also include a term or terms C' favouring the smoothness (in some sense) of the amplitude distribution so as to minimize distortion caused by mutual coupling among the elements (a term widely used for this purpose is $b\left(DRR_d - DRR\right)^2$, where DRR is the dynamic range ratio $|I_{\max}/I_{\min}|$ of the excitations and b is a weighting factor):

$$C = \sum_{p=1}^{P} C_p + C' \quad (3)$$

3. EXAMPLES

We consider a 16×16 square array of elements spaced $\lambda/2$ apart in both the *x* and *y* directions that is required to generate a sum pattern with a beamwidth of 7.7° at the level of the side lobes, a circular footprint and a square footprint (the size, location and rolloff margins of the footprints are specified in Fig.1). Because of the array size and spacing, eq.1 becomes

$$F(u,v) = \sum_{m,n=-L}^{L-1} I_{mn} \exp\left\{ j\frac{\pi}{2}\left[(2m+1)u + (2n+1)v\right]\right\} \tag{4}$$

where $u=\sin\theta\cos\varphi$, $v=\sin\theta\sin\varphi$, and $L=16/2=8$; and because all the patterns have eight-fold symmetry, this can be further simplified to

$$F(u,v) = \sum_{m=1}^{L}\sum_{n=m}^{L} I_{mn}\,\varepsilon_{mn}\left(V_{mn} + V_{nm}\right) \tag{5}$$

where

$$V_{mn} = \cos\left(\frac{(2m-1)\pi\, u}{2}\right)\cos\left(\frac{(2n-1)\pi\, v}{2}\right) \tag{6a}$$

$$V_{nm} = \cos\left(\frac{(2n-1)\pi\, u}{2}\right)\cos\left(\frac{(2m-1)\pi\, v}{2}\right) \tag{6b}$$

and ε_{mn} is unity except when $n=m$, in which case $\varepsilon_{mm} = 1/2$.

We present three solutions to the above problem: one in which a uniform excitation amplitude distribution is imposed; one in which the imposed amplitude distribution is obtained by sampling a Gaussian surface,

$$I_{mn} = \exp\left\{-0.8\left(\alpha_m^2 + \beta_n^2\right)\right\} \tag{7}$$

where $\alpha_m = (2m-1)/(2L-1)$, $\beta_n = (2n-1)/(2L-1)$ and the coefficient 0.8 is calculated so that the dynamic range ratio is approximately 5; and one in which the amplitude distribution is

optimized jointly with the three phase distributions subject only to the condition that the dynamic range ratio must be less than 20. The first two solutions were obtained using eq.2 for the cost functions (with the ripple term omitted for the sum patterns), and the third using eq.3 with $C' = b\left(DRR_d - DRR\right)^2$. For each condition on the excitation amplitude distribution, the maximum sidelobe and ripple levels of the three patterns are listed in Table I (the ripple values are half the peak-to-trough differences), together with the time taken to obtain the solution using a computer with an AMD-K6-2 processor operating at 500 MHz.

Figs.2a-c show the patterns obtained when a uniform excitation amplitude distribution was imposed. Satisfactory ripple levels were obtained for the footprints (±0.1-0.2 dB), and a satisfactory sidelobe level for the sum pattern (-21 dB), but the condition on the excitation amplitudes is too strict to allow sidelobe levels lower than -9 dB to be achieved for the footprints. Better footprint sidelobe levels of -14 and -15 dB were attained with the Gaussian amplitude distribution without significantly affecting either the sidelobe level of the sum pattern or the ripple levels of the footprints. Fig.3 shows the patterns obtained.

Finally, joint optimization of the excitation amplitudes and phases afforded footprints with sidelobe levels of approximately -19 or -20 dB at the cost of a rise in the sum pattern sidelobe level of only 2 dB while keeping footprint ripple below ±0.25 dB. The dynamic range ratio of the solution obtained is 14.9. Fig.4 shows the three patterns, and Table II lists the excitation amplitudes and phases.

Note that the execution time for the joint-optimization solution was about the same as the total execution times of the prefixed-amplitude solutions, in spite of the number of simultaneously optimized quantities being four times as large. These times of course depend heavily on the

number of points at which the pattern is calculated; in this work the pattern was calculated on a grid of 60×60 points in the (u,v) plane.

4. CONCLUSIONS

Simulated annealing can achieve the synthesis of multi-pattern planar arrays with fixed excitation amplitude distributions. The amplitude distribution may be prefixed, or optimized jointly with the pattern-specific phase distributions subject to appropriate smoothness constraints. Computations can be carried out within reasonable times on conventional desktop computers.

Acknowledgement. This work was supported by the Xunta de Galicia under project PGIDT00PXI20603PR

REFERENCES

1. M. Dürr, A. Trastoy, and F. Ares, Multiple pattern linear antenna arrays with single prefixed amplitude distributions: modified Woodward-Lawson synthesis, Electronics Letters, Vol. 36, No. 16, (2000), 1345-1346.

2. X. Díaz, J. A. Rodríguez, F. Ares and E. Moreno, Design of phase-differentiated multiple-pattern antenna arrays, Microwave and Optical Tecnology Letters, Vol. 26, No. 1, (2000), 53-54.

3. O. M. Bucci, G. Mazzarella, and G. Panariello, Reconfigurable Arrays by Phase-Only Control, IEEE Trans. Antennas Propagat., Vol. 39, No. 7, (1991), 919-925.

4. W. H. Press, S. A. Teukolsky, W. T. Vetterling and B. P. Flannery, Numerical Recipes in C, Cambridge University Press, (1992), 444-455.

LEGENDS FOR TABLES

Table I. Sidelobe levels, ripple (half peak-to-trough distance) and computation times of each pattern obtained under each condition on the excitation amplitude distribution.

Table II. Jointly optimized excitation amplitudes and phases for the three patterns (one quadrant of the array is shown).

LEGENDS FOR FIGURES

Fig.1. Boundaries defining the base and top perimeters of the circular (a) and square (b) footprint patterns.

Fig.2. Sum (a), circular footprint (b) and square footprint (c) patterns obtained imposing a uniform excitation amplitude distribution. $G'(u,v) = 20 \log(|F(u,v)|/|F(u,v)|_{max})$.

Fig.3. As for Fig.2, but for a Gaussian excitation amplitude distribution.

Fig.4. As for Fig.2, but with an excitation amplitude distribution optimized jointly with the three excitation phase distributions.

Amplitude distribution	Pattern	SLL (dB)	Ripple (dB)	Computer time (s)
Uniform	Sum	-20.9	-	206
	Circular	-9.0	0.20	207
	Square	-9.0	0.11	222
Gaussian	Sum	-20.7	-	169
	Circular	-14.0	0.20	178
	Square	-15.0	0.13	156
Jointly Optimized	Sum	-18.8	-	624
	Circular	-19.2	0.23	
	Square	-19.9	0.18	

Table I

n \ m	1	2	3	4	5	6	7	8
Amplitudes								
8	0.135	0.141	0.125	0.104	0.104	0.105	0.078	0.074
7	0.154	0.140	0.117	0.117	0.069	0.112	0.082	0.078
6	0.329	0.269	0.184	0.157	0.102	0.107	0.112	0.105
5	0.394	0.328	0.258	0.204	0.159	0.102	0.069	0.104
4	0.420	0.362	0.268	0.271	0.204	0.157	0.117	0.104
3	0.442	0.352	0.348	0.268	0.258	0.184	0.117	0.125
2	0.834	0.608	0.352	0.362	0.328	0.269	0.140	0.141
1	1.000	0.834	0.442	0.420	0.394	0.329	0.154	0.135
Phases for sum pattern (deg.)								
8	-161.430	-170.672	-164.318	-168.838	-170.667	-165.796	-158.818	-114.597
7	-171.480	-171.181	-162.021	-151.288	-151.232	-155.431	-140.386	-158.818
6	-151.656	-155.603	-155.328	-157.270	-160.422	-149.993	-155.431	-165.796
5	-166.151	163.958	-175.428	-152.555	-167.446	-160.422	-151.232	-170.667
4	-155.128	-142.975	147.433	154.980	-152.555	-157.270	-151.288	-168.838
3	162.893	9.649	-156.136	147.433	-175.428	-155.328	-162.021	-164.318
2	-135.842	-139.061	9.649	-142.975	163.958	-155.603	-171.181	-170.672
1	60.940	-135.842	162.893	-155.128	-166.151	-151.656	-171.480	-161.430
Phases for circular footprint (deg.)								
8	118.580	112.707	71.872	58.786	78.662	39.752	-64.388	-132.742
7	-59.421	177.967	133.488	120.883	134.674	106.645	13.843	-64.388
6	-142.024	-123.094	-149.708	174.260	131.013	123.467	106.645	39.752
5	-107.234	-123.306	-129.465	-159.305	-178.298	131.013	134.674	78.662
4	-97.907	-103.957	-117.845	-126.342	-159.305	174.260	120.883	58.786
3	-15.670	-76.346	-80.363	-117.845	-129.465	-149.708	133.488	71.872
2	-1.346	-0.635	-76.346	-103.957	-123.306	-123.094	177.967	112.707
1	12.090	-1.346	-15.670	-97.907	-107.234	-142.024	-59.421	118.580
Phases for square footprint (deg.)								
8	107.694	127.169	-173.990	-114.608	145.056	-113.674	-21.629	-39.459
7	3.450	33.450	84.856	158.417	32.235	54.455	-173.244	-21.629
6	-18.151	-22.723	25.543	94.373	121.840	112.616	54.455	-113.674
5	-37.677	-32.543	-4.090	68.326	78.421	121.840	32.235	145.056
4	-65.024	-54.247	-29.314	22.082	68.326	94.373	158.417	-114.608
3	-116.917	-101.785	-80.872	-29.364	-4.090	25.543	84.856	-173.990
2	-148.716	-132.966	-101.785	-54.247	-32.543	-22.723	33.450	127.169
1	-159.620	-148.716	-116.917	-65.024	-37.677	-18.151	3.450	107.694

Table II

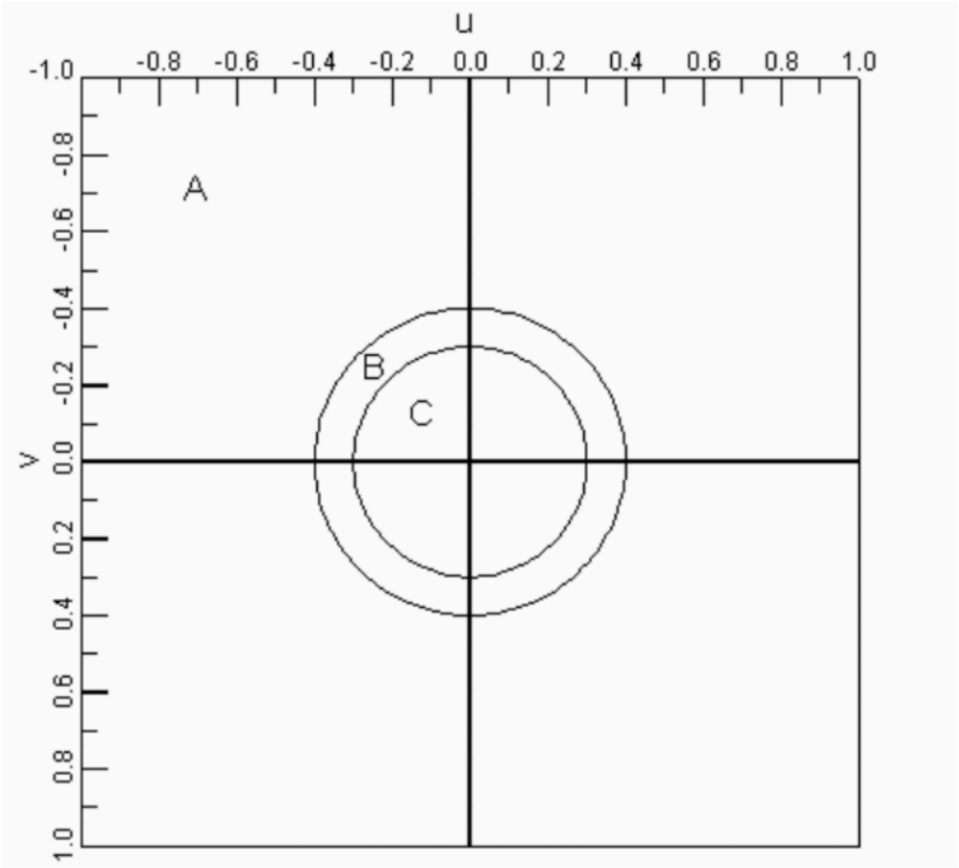

Fig.1a

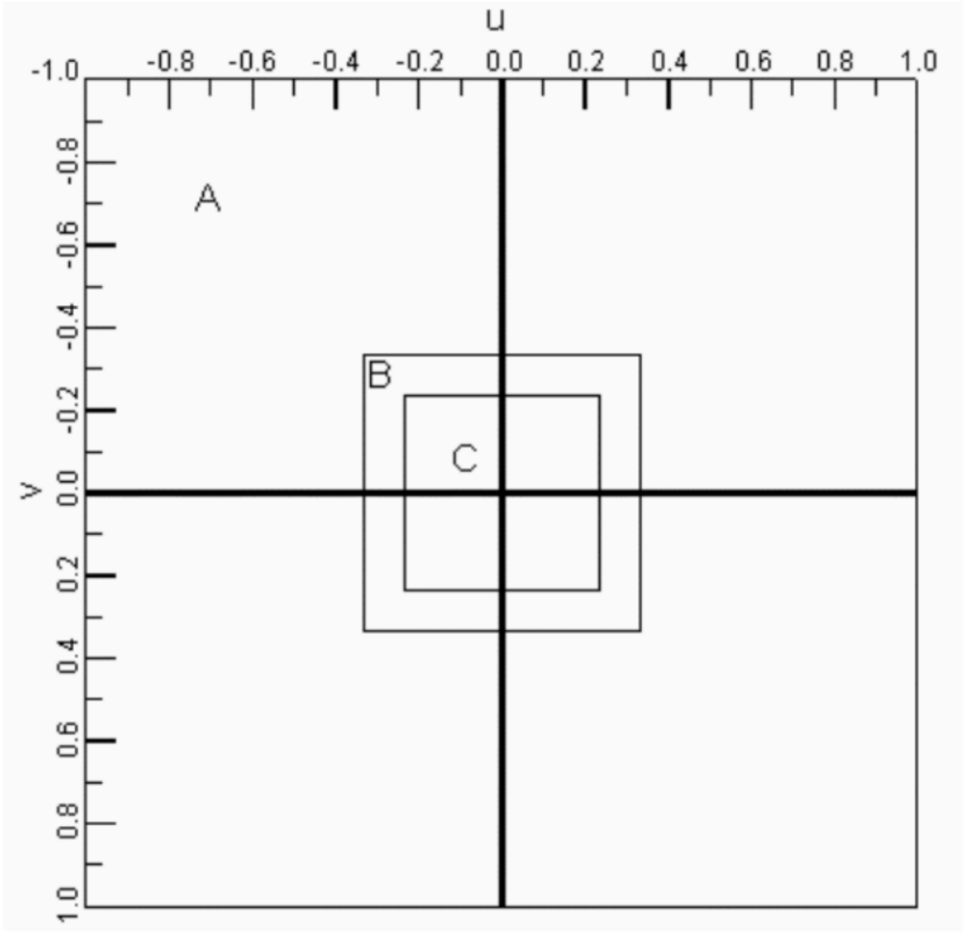

Fig.1b

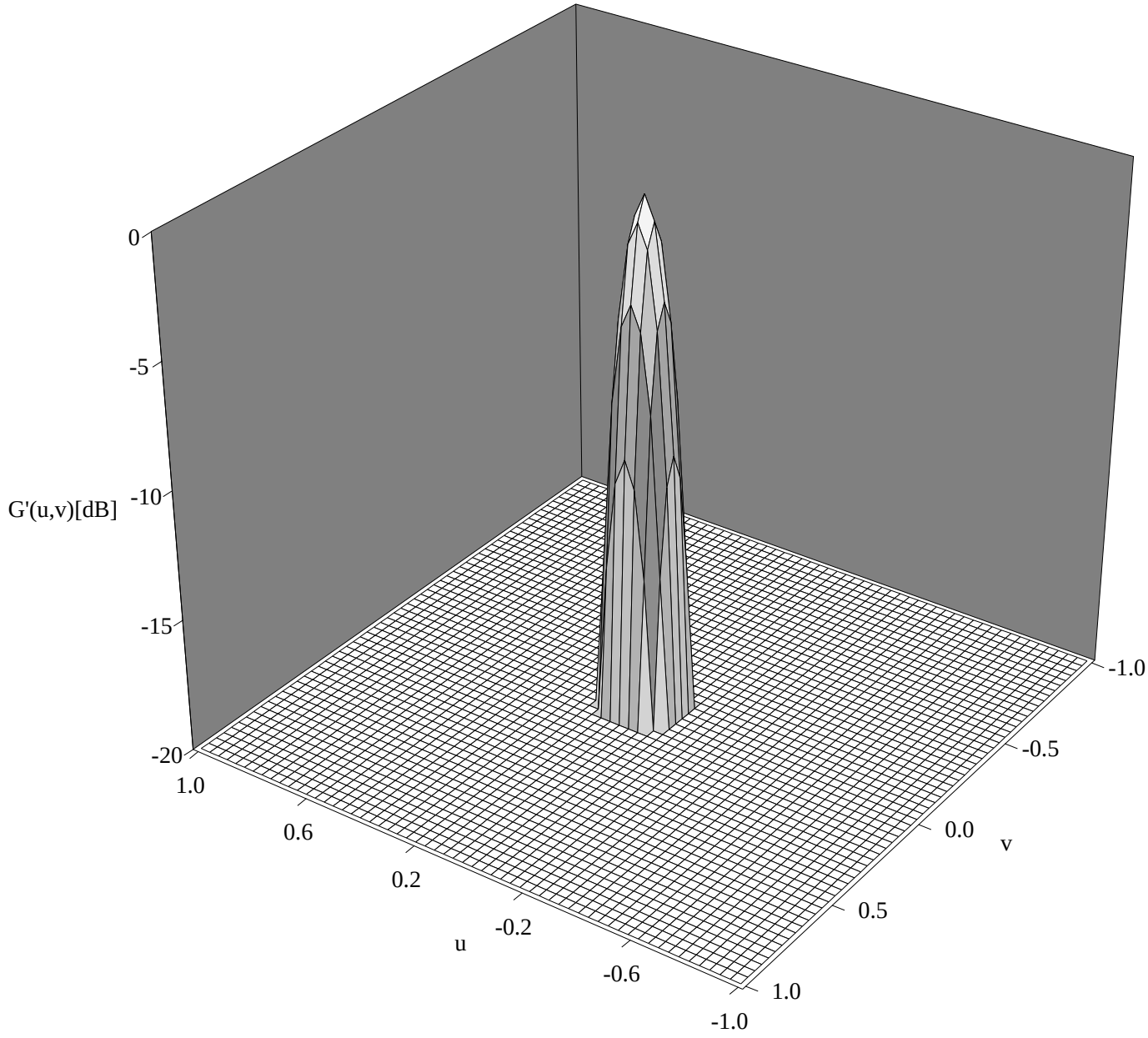

Fig 2a.

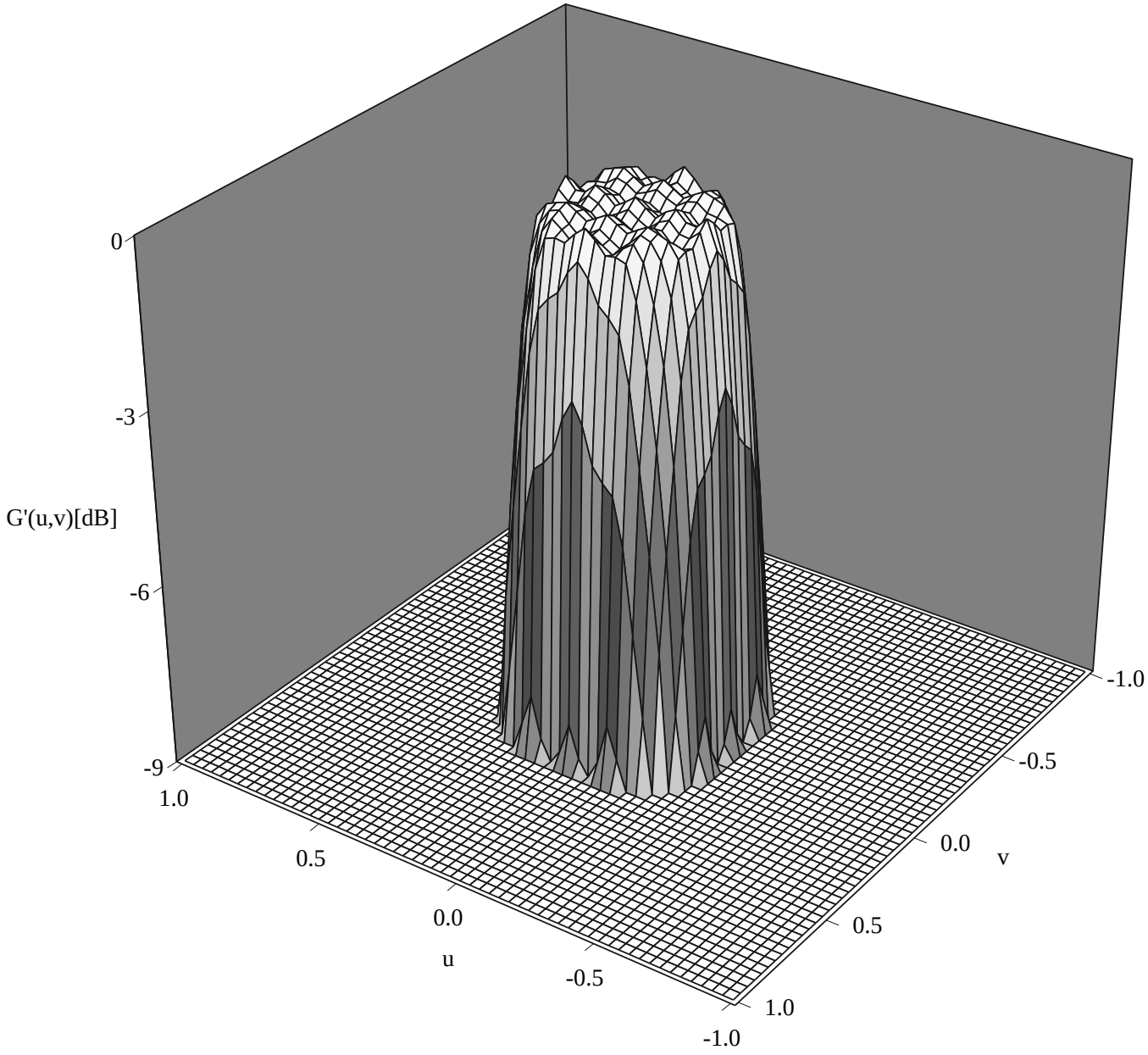

Fig 2b

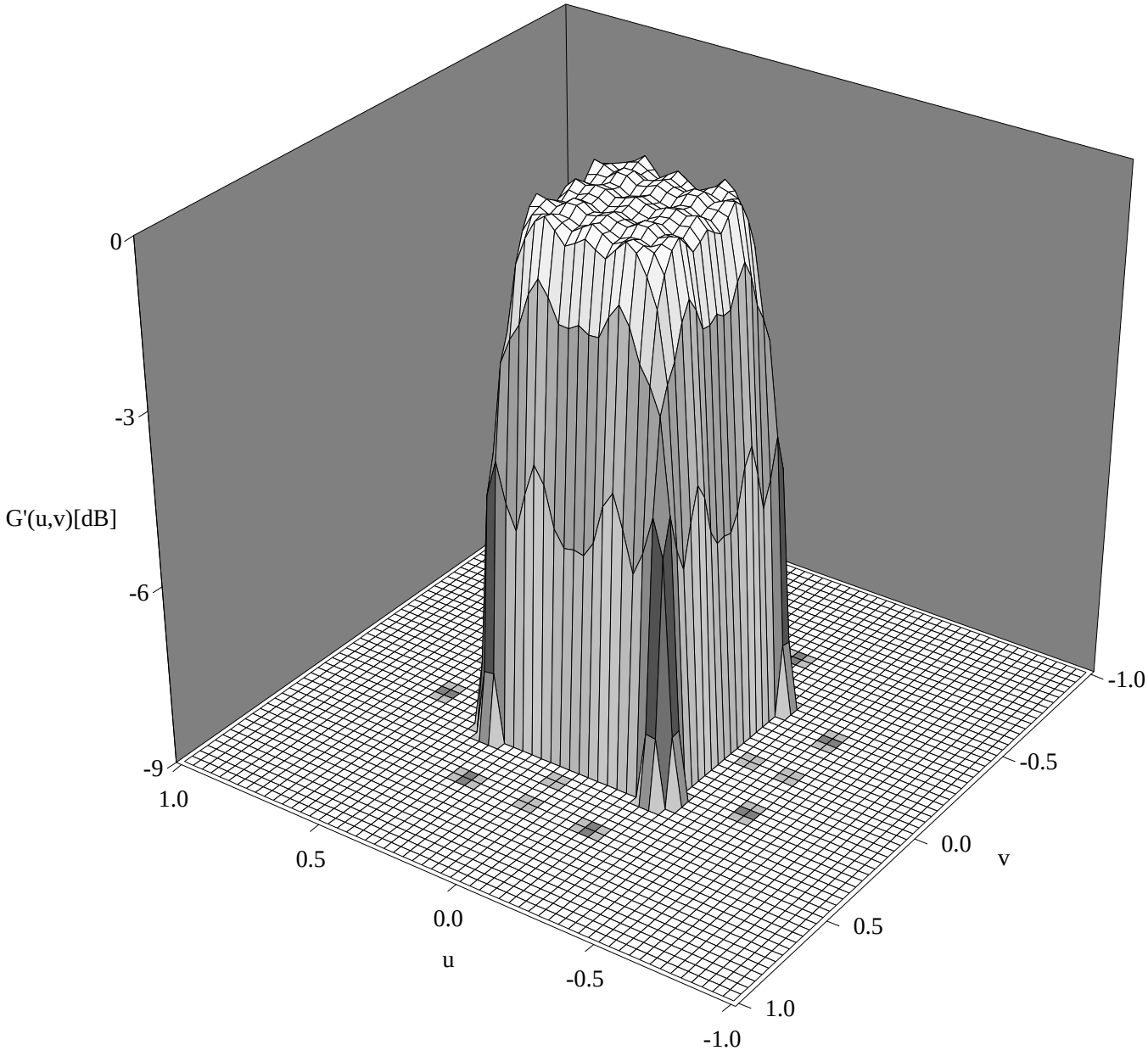

Figs.2c

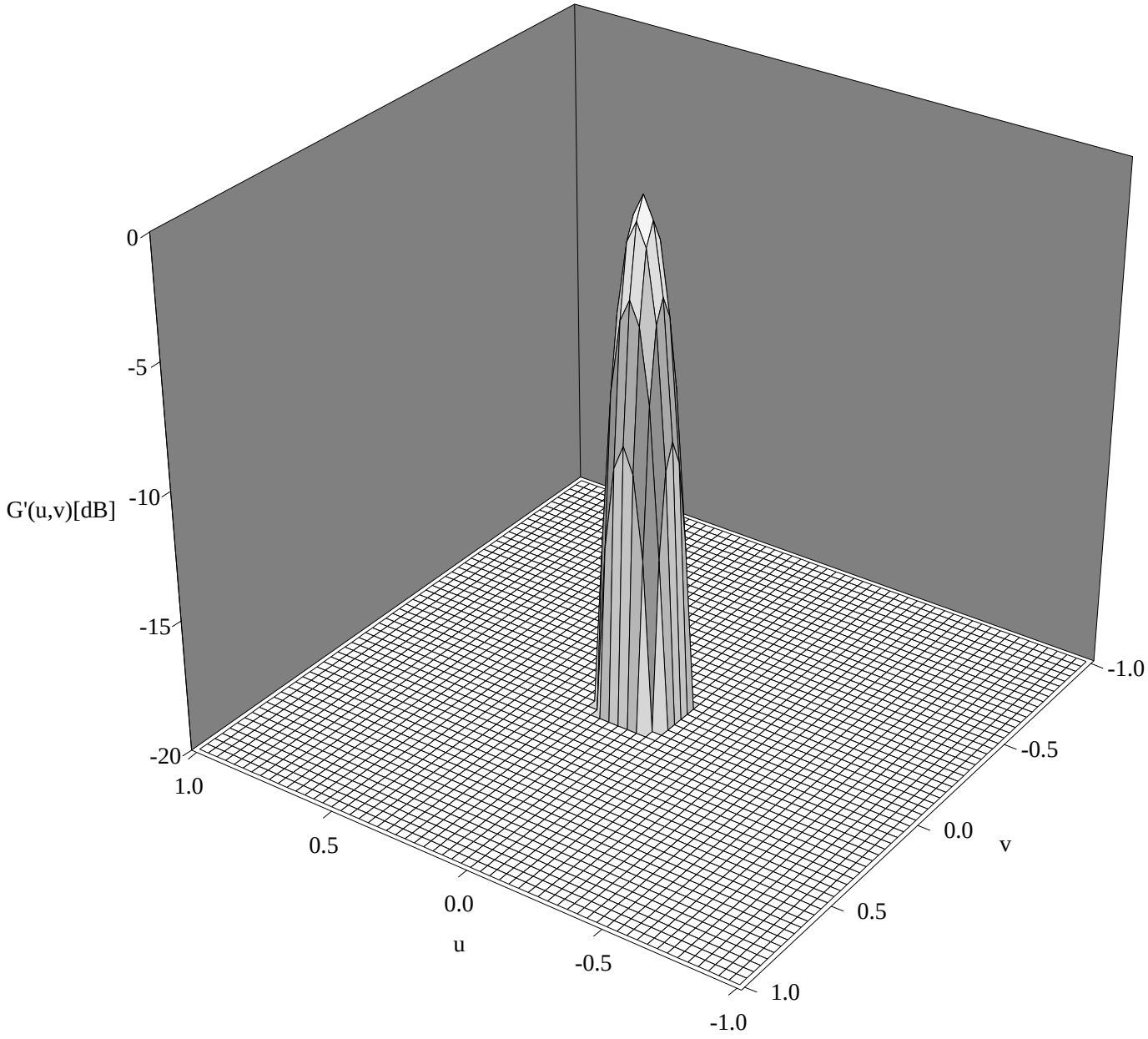

Fig.3a

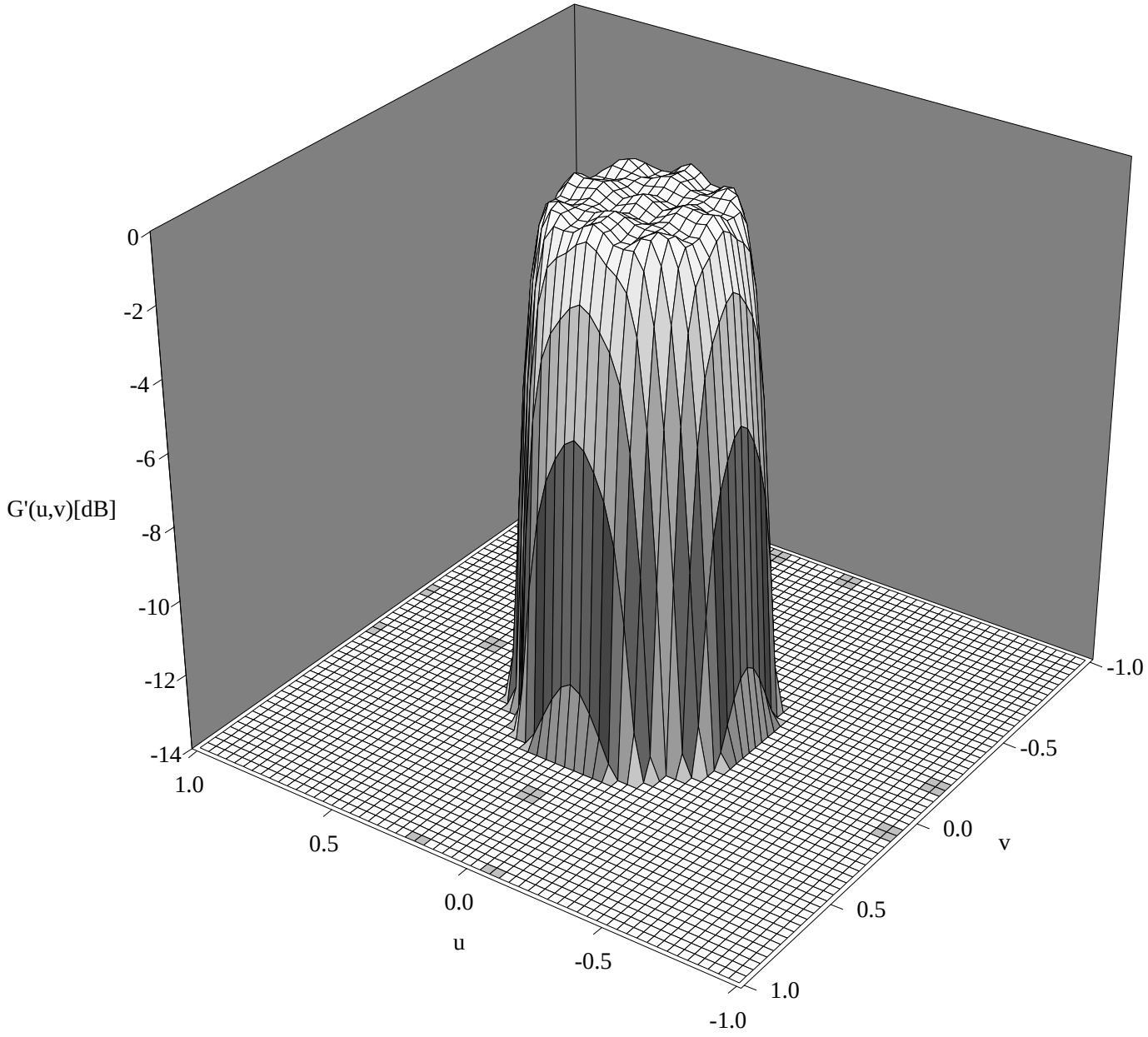

Fig.3b

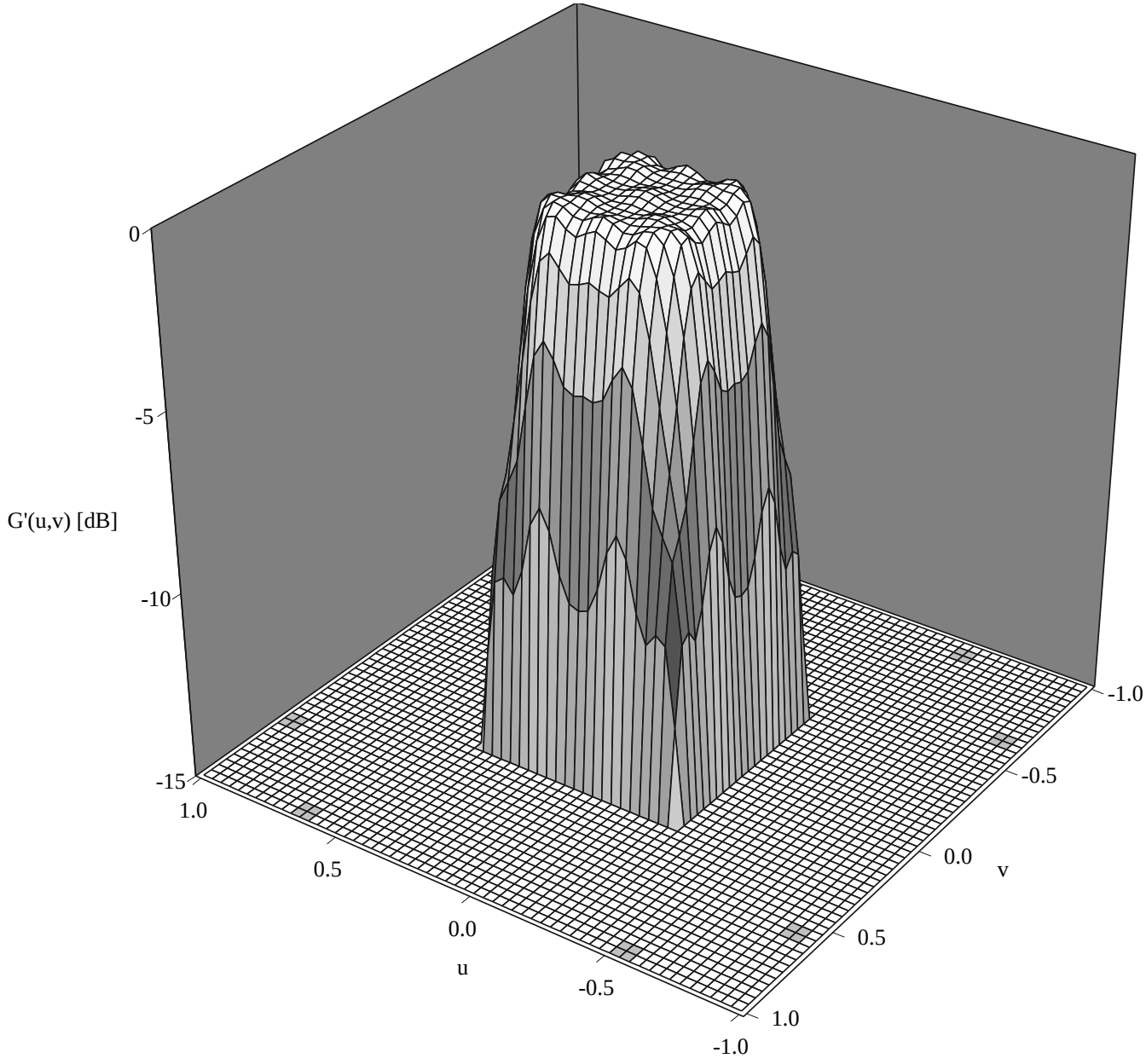

Fig.3c

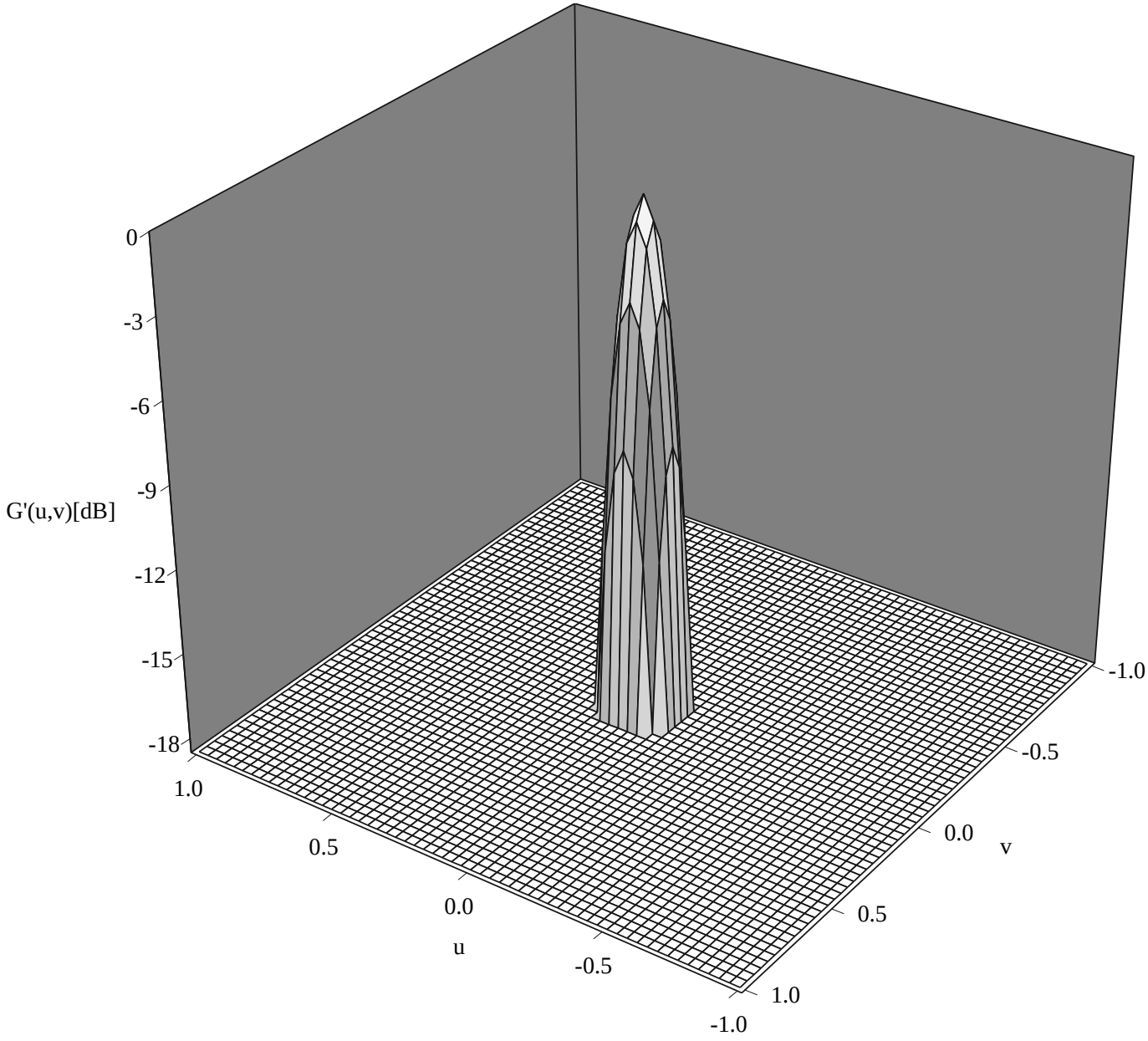

Fig.4a

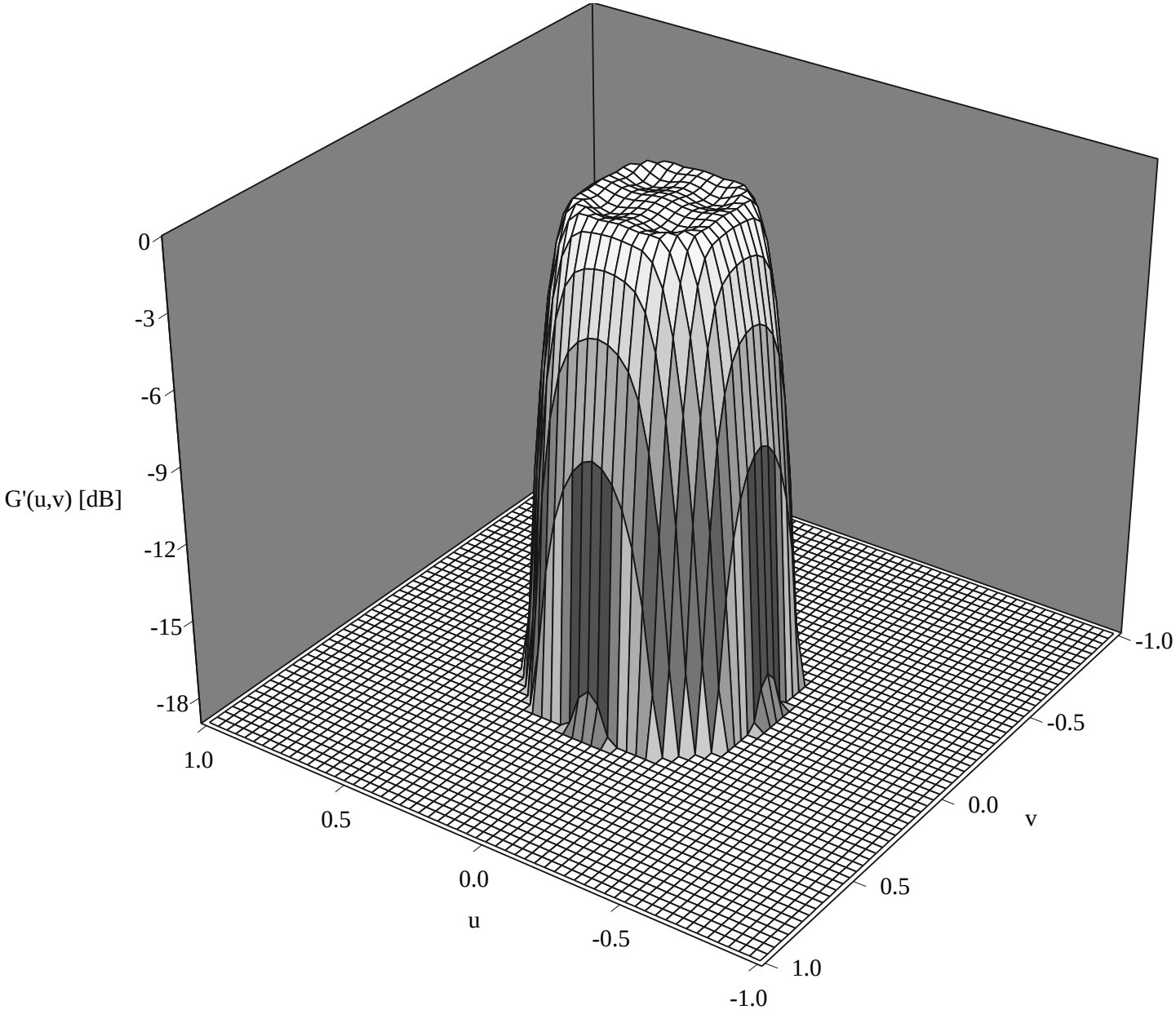

Fig.4b

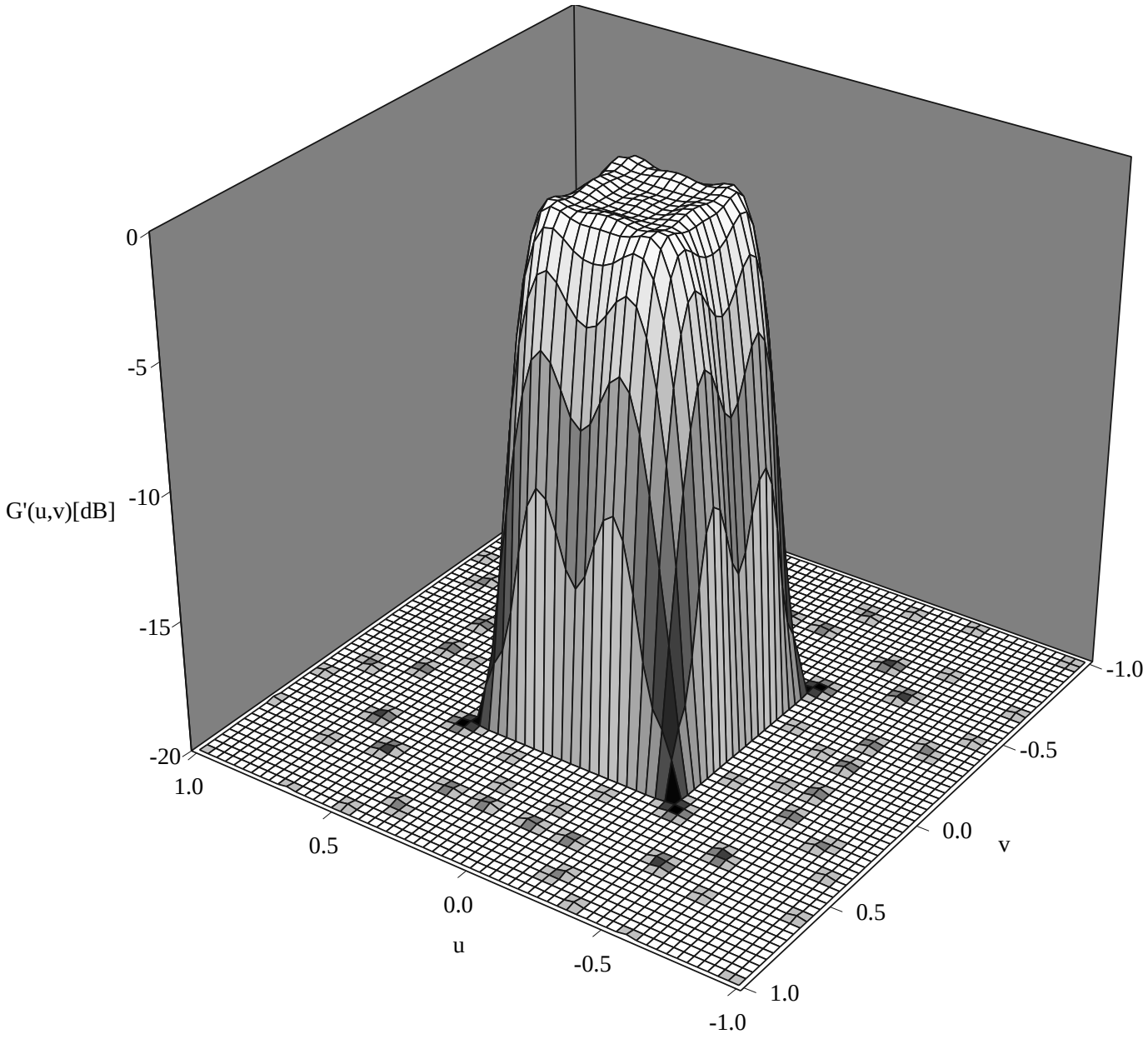

Fig.4c